# A Two-Dimensional Signal Space for Intensity-Modulated Channels

# A Two-Dimensional Signal Space for Intensity-Modulated Channels

Johnny Karout, *Student Member, IEEE,* Gerhard Kramer, *Fellow, IEEE,* Frank R. Kschischang, *Fellow, IEEE,* and Erik Agrell

***Abstract*—A two-dimensional signal space for intensity-modulated channels is presented. Modulation formats using this signal space are designed to minimize average and peak power for a fixed minimum distance between signal points. The uncoded, high-signal-to-noise ratio, power and spectral efficiencies are compared to those of the best known formats. The new formats are simpler than existing subcarrier formats, and are superior if the bandwidth is measured as 90% in-band power. Existing subcarrier formats are better if the bandwidth is measured as 99% in-band power.**

***Index Terms*—Direct detection, intensity modulation, noncoherent communications, power efficiency, spectral efficiency.**

## I. Introduction

INTENSITY modulation with direct detection (IM/DD) is widespread for low-cost optical communication systems, e.g., wireless optical links [1]–[3] and short-haul fiber links [4]. IM/DD permits only the intensity of light to carry information. In contrast, coherent optical systems such as long-haul fiber links let data modulate the optical carrier's amplitude and phase via, e.g., $M$-ary quadrature amplitude modulation ($M$-QAM). Designing IM/DD formats with good power and spectral characteristics is challenging [1], [2], [5]–[7].

In the absence of optical amplification, IM/DD systems can be modeled as additive white Gaussian noise (AWGN) channels with nonnegative inputs [1, Ch. 5], [2], [5], [8, Sec. 11.2.3]. Nonnegative $M$-ary pulse amplitude modulation ($M$-PAM) such as on-off keying (OOK) [1, Eq. (5.8)] is a natural modulation format but it is power inefficient for $M > 2$ [9]. Subcarrier modulation (SCM) allows using $M$-QAM by adding a direct current (DC) bias to the electrical signal to make it nonnegative [1, Ch. 5]. The DC bias does not carry information if it is independent of the transmitted information. A signal space for IM/DD channels was presented in [5] and power-efficient subcarrier modulation formats were designed. In our prior work, a three-dimensional signal space for IM/DD, whose signal sets are denoted as raised-QAM [5], was used to numerically optimize modulation formats for different power constraints [6], [7].

J. Karout and E. Agrell are with the Department of Signals and Systems, Chalmers University of Technology, SE-412 96 Gothenburg, Sweden (johnny.karout, agrell@chalmers.se).

G. Kramer is with the Institute for Communications Engineering, Technische Universität München, D-80290 Munich, Germany (gerhard.kramer@tum.de).

F. R. Kschischang is with the Edward S. Rogers Sr. Department of Electrical and Computer Engineering, University of Toronto, Toronto, ON M5S 3G4, Canada (e-mail: frank@comm.utoronto.ca). His work was performed while on a Fellowship at the Institute for Advanced Study, Technische Universität München, Lichtenbergstrasse 2a, D-85748 Garching, Germany.

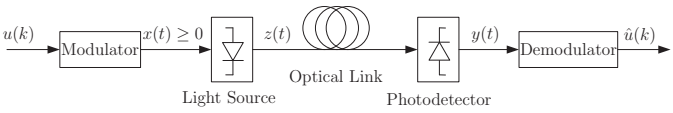


Fig. 1. Passband transceiver of IM/DD systems.

In this work, we present a two-dimensional signal space for optical IM/DD systems. The resulting modulation formats have simpler modulator and demodulator structures than the three-dimensional formats studied before. Their power and spectral efficiencies are evaluated and compared to the previously best known formats.

## II. System Model

Consider an AWGN channel whose input $x(t)$ is nonnegative. The symbols $u(k)$, for $k = \ldots, -1, 0, 1, \ldots$, are independent and uniformly distributed over $\{0, 1, \ldots, M-1\}$. The modulator maps each $u(k)$ to a real and nonnegative waveform belonging to the signal set $S = \{s_0(t), s_1(t), \ldots, s_{M-1}(t)\}$, where $s_i(t) = 0$ for $t \notin [0, T)$, $i = 0, 1, \ldots, M-1$, and $T$ is the symbol period. The transmitted waveform is

$$x(t) = \sum_{k=-\infty}^{\infty} s_{u(k)}(t - kT). \tag{1}$$

The received signal is modeled as

$$y(t) = x(t) + n(t), \tag{2}$$

where $n(t)$ is a zero-mean white Gaussian process with double-sided power spectral density $N_0/2$. The demodulator is a correlator or matched filter receiver with a minimum-distance detector, i.e., it minimizes the symbol error rate at a given signal-to-noise (SNR) ratio [10, Sec. 4.1] and puts out $\hat{u}(k)$ as the estimate of $u(k)$.

The AWGN model is reasonable for wireless IM/DD systems under the assumption that the channel is nondistorting in the frequency range of interest [1, Ch. 5], [2], [5], and for short-haul fiber links with negligible dispersion[1] and when the dominating noise is from the receiver itself, and not from optical amplifiers [8, Sec. 11.2.3], [11, p. 155]. In Sec. III-A, power constraints are imposed on $x(t)$ to reflect some of the physical characteristics of the IM/DD channel. A passband model for IM/DD systems is depicted in Fig. 1. The electrical

[1]For an OM3+ graded index multimode fiber (MMF), the bandwidth–distance product is 4.7 GHz·km. This means, roughly, that MMF links can be considered dispersion-free at 10 Gbaud if their length is much shorter than 470 m.

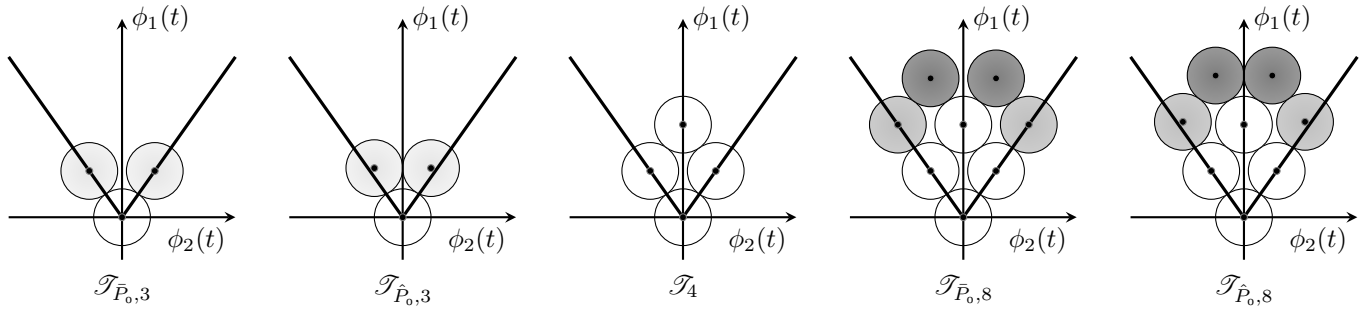


Fig. 2. Two-dimensional constellations optimized for average and peak optical power. Circles which are different between constellations of the same size are shaded differently. The coordinates of these constellations are listed in Appendix A.

nonnegative waveform $x(t)$ modulates a light source such as a laser diode. The information is carried by the intensity of the passband signal

$$z(t) = \sqrt{2cx(t)}\cos(2\pi f_\mathrm{o} t + \theta(t)), \tag{3}$$

where $c$ represents the electro-optical conversion factor in watts per ampere (W/A) [12], $f_\mathrm{o}$ is the optical carrier frequency, and $\theta(t)$ is a random phase, uniformly distributed in $[0, 2\pi)$ and varying slowly with $t$ relative to the symbol rate. The optical signal propagates through the optical medium depicted as an optical fiber in Fig. 1, but which could also be a free-space optical link. The photodetector at the receiver, with responsivity $r$ in A/W, detects the intensity of $z(t)$. Without loss of generality, $c$ and $r$ are normalized so that the received electrical signal $y(t)$ can be written as (2) [11, p. 155].

## III. Signal Space Analysis

The signals in $S$ can be represented as $s_i(t) = \sum_{k=1}^{N} s_{i,k}\,\phi_k(t)$ for $i = 0, \ldots, M-1$, where $\{\phi_k(t)\}_{k=1}^{N}$, $N \leq M$, is a set of orthonormal basis functions [5]. The vector representation of $s_i(t)$ with respect to these basis functions is $\mathbf{s}_i = (s_{i,1}, s_{i,2}, \ldots, s_{i,N})$. We may thus alternatively represent the signal set as $S = \{\mathbf{s}_0, \mathbf{s}_1, \ldots, \mathbf{s}_{M-1}\}$.

Consider a two-dimensional signal space for IM/DD spanned by the basis functions

$$\phi_1(t) = \sqrt{\frac{1}{T}}\ \mathrm{rect}\left(\frac{t}{T}\right), \tag{4}$$

$$\phi_2(t) = \sqrt{\frac{2}{T}}\ \cos(2\pi f t)\ \mathrm{rect}\left(\frac{t}{T}\right), \tag{5}$$

where $\mathrm{rect}(t/T) = 1$ for $t \in [0, T)$ and 0 elsewhere, and the electrical subcarrier frequency $f = 1/2T$. In [5] and our prior work [6], [7], a three-dimensional signal space with signal sets called raised-QAM was used to design modulation formats. This three-dimensional signal space is spanned by $\phi_1(t)$ in (4), and the in-phase and quadrature phase modulation formats' basis functions with $f = 1/T$ [7, Eqs. (13)–(14)]. The basis function $\phi_1(t)$ represents the DC bias, and is used as in [5] to guarantee signal nonnegativity.

We follow the same steps as in Theorem 1 in [7] for raised-QAM. The admissible region $\Upsilon$, defined as the set of two-dimensional signal vectors satisfying a nonnegativity constraint, is a two-dimensional cone with vertex at the origin, an apex angle of $\cos^{-1}(1/3) = 70.528°$, and an opening in the dimension spanned by $\phi_1(t)$.

### A. Example Modulation Formats

Fig. 2 presents several modulation formats designed for the admissible region $\Upsilon$. The constellation points, regarded as the centers of circles with diameter equal to the minimum distance, are placed in $\Upsilon$ such that they minimize a certain power criterion. As in [5], [7], the average optical power

$$\bar{P}_\mathrm{o} = \lim_{T\to\infty} \frac{1}{2T}\int_{-T}^{T} z^2(t)\,\mathrm{d}t = \lim_{T\to\infty} \frac{c}{2T}\int_{-T}^{T} x(t)\,\mathrm{d}t, \tag{6}$$

and peak optical power

$$\hat{P}_\mathrm{o} = \max_t \frac{z^2(t)}{2} = c \max_t x(t) \tag{7}$$

are used as design criteria. The modulation formats numerically optimized for average optical power are denoted as $\mathscr{T}_{\bar{P}_\mathrm{o},M}$, and for peak optical power as $\mathscr{T}_{\hat{P}_\mathrm{o},M}$. They are listed in Appendix A. $\mathscr{T}_4$ is a 4-ary constellation optimized for both power measures. Together with $\mathscr{T}_{\bar{P}_\mathrm{o},3}$ and $\mathscr{T}_{\bar{P}_\mathrm{o},8}$, they are subsets of a lattice where the angle between its two basis vectors is $\cos^{-1}(1/3)$, which is the apex angle of the cone.

### B. Performance Measures

To evaluate performance, the uncoded and asymptotic (high-SNR) power gains with respect to OOK are considered [1], [2], [7]. The average optical power gain $\bar{P}_{\mathrm{o,\,gain}}$ over OOK for the same error rate performance is defined in [7, Eq. (32)], and the peak optical power gain $\hat{P}_{\mathrm{o,\,gain}}$ with respect to OOK is defined in [7, Eq. (33)]. The average optical power is an important figure of merit for skin- and eye-safety in wireless optical links [1, Ch. 5], [2], [5], and the peak power measures tolerance against nonlinearities [13].

The spectral efficiency measures the bit rate achieved in a given bandwidth. It is defined as

$$\eta = \frac{R_\mathrm{b}}{W}\ \text{[bit/s/Hz]}, \tag{8}$$

where $R_\mathrm{b} = (1/T)\log_2 M$ is the bit rate, and $W$ is the baseband bandwidth of $x(t)$. In [1], [6], [7], $W$ was defined as the first null in the spectrum, i.e., the width of the main lobe, since most of the energy of a signal is contained in this main lobe. However, some modulation formats designed using the signal space in Sec. III have no spectral nulls. Fig. 2 shows five formats that lack spectral nulls. This makes this definition of bandwidth misleading. Instead, as in [3, p. 49], we will use the fractional power bandwidth $W$ defined as the length of

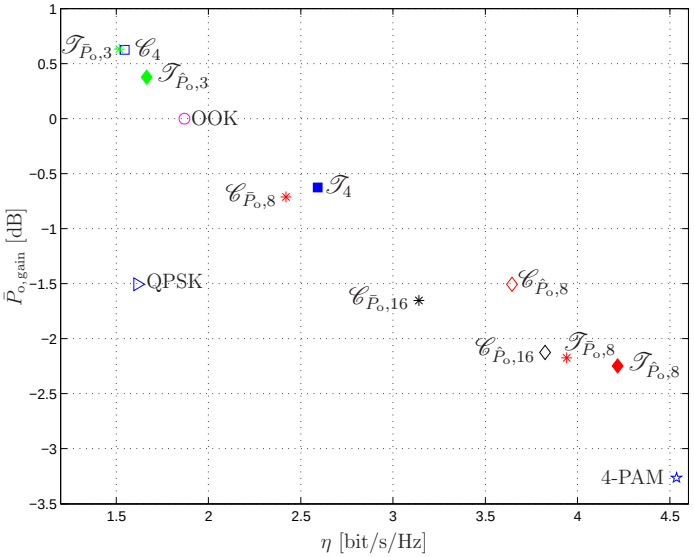


Fig. 3. Asymptotic average optical power gain of modulation formats over OOK ($K = 0.9$). ($\mathscr{T}$ refers to two-dimensional constellations in Fig. 2 and $\mathscr{C}$ refers to three-dimensional constellations in [7]. Further, constellations of the same size have the same marker color.)

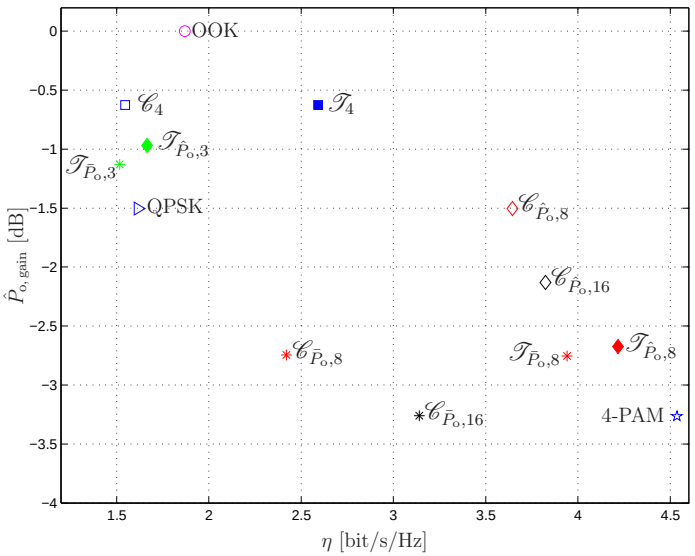


Fig. 4. Asymptotic peak optical power gain of modulation formats over OOK ($K = 0.9$).

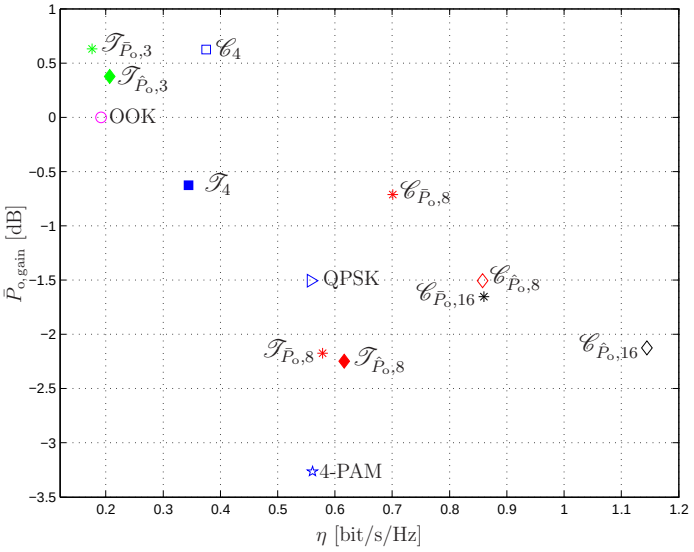


Fig. 5. Asymptotic average optical power gain of modulation formats over OOK ($K = 0.99$).

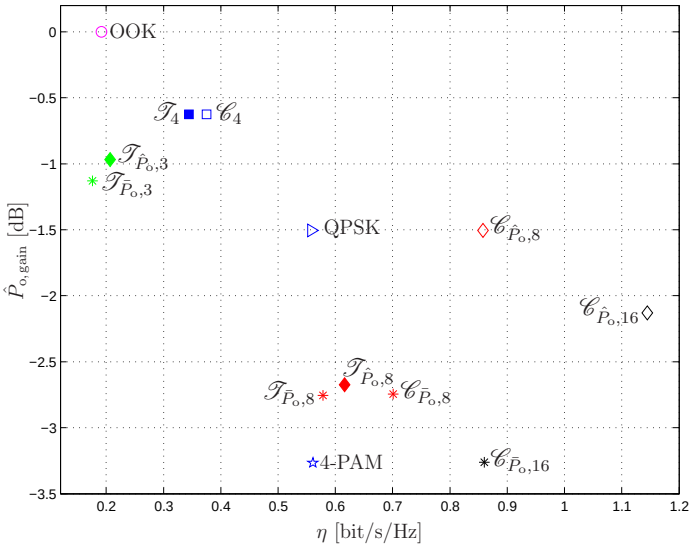


Fig. 6. Asymptotic peak optical power gain of modulation formats over OOK ($K = 0.99$).

the smallest frequency interval carrying a certain fraction of the total power. Note, however, that [3, Eq. (3.15)] accounts only for the continuous spectrum of $x(t)$. We will include both the discrete and continuous spectrum as in [14]. For IM/DD channels, the discrete spectral component at $f = 0$ (at DC) represents the average optical power of a constellation [3, p. 47]. The fractional power bandwidth $W$ is the solution to

$$\frac{\int_{-W}^{W} S_x(f)\,\mathrm{d}f}{\int_{-\infty}^{\infty} S_x(f)\,\mathrm{d}f} = K, \tag{9}$$

where $S_x(f)$ is the power spectral density of $x(t)$, and $K \in (0, 1)$. Specifically, $W$ is reduced if a DC bias is added to the signal. The power spectral density depends on the choice of basis functions, constellation points, and the correlation between symbols. For constellations with uniform probability distribution, $S_x(f)$ can be obtained using [15, Eq. (3.7.6)], which is evaluated using only the Fourier transform of the signals in $S$.

## IV. Performance Analysis

Figs. 3–6 depict the (uncoded, high-SNR) average and peak optical power gains of our modulation formats with respect to OOK, and as a function of spectral efficiency $\eta$. The fractional power bandwidth $W$ was computed using $K = 0.9$ and $K = 0.99$, which are somewhat arbitrary but commonly used.

In addition to the modulation formats introduced in this paper, we consider subcarrier QPSK, nonnegative 4-PAM, and three-dimensional modulation formats from previous work optimized for average optical power ($\mathscr{C}_{\bar{P}_\mathrm{o},M}$) and peak optical power ($\mathscr{C}_{\hat{P}_\mathrm{o},M}$) [7]. We next discuss the plots in Figs. 3–6.

*1) $\bar{P}_{\mathrm{o,gain}}$ vs. $\eta$ with $K = 0.9$ (Fig. 3):* For a fixed $M$, modulation formats optimized for average power have a

larger $\bar{P}_{\text{o, gain}}$ than those optimized for peak power. The three-dimensional constellation optimized for both power measures, $\mathscr{C}_4$, has a similar $\eta$ and $\bar{P}_{\text{o, gain}}$ as $\mathscr{T}_{\bar{P}_{\text{o}},3}$, whereas $\mathscr{T}_4$ has better power and spectral efficiency than $\mathscr{C}_{\bar{P}_{\text{o}},8}$. The three-dimensional constellations optimized for peak power, $\mathscr{C}_{\hat{P}_{\text{o}},8}$ and $\mathscr{C}_{\hat{P}_{\text{o}},16}$, have higher $\eta$ than $\mathscr{C}_{\bar{P}_{\text{o}},8}$ and $\mathscr{C}_{\bar{P}_{\text{o}},16}$. This comes at the price of a lower power efficiency. $\mathscr{T}_{\hat{P}_{\text{o}},8}$ has a higher $\eta$ than $\mathscr{T}_{\bar{P}_{\text{o}},8}$, and 4-PAM has the highest $\eta$ and lowest $\bar{P}_{\text{o, gain}}$. For $K = 0.9$, the modulation formats designed using the two-dimensional signal space have better spectral-efficiency characteristics than formats designed using raised-QAM. For example, $\mathscr{T}_{\hat{P}_{\text{o}},8}$ has a better $\eta$ than $\mathscr{C}_{\hat{P}_{\text{o}},16}$.

*2) $\hat{P}_{\text{o, gain}}$ vs. $\eta$ with $K = 0.9$ (Fig. 4):* For a fixed $M$, modulation formats optimized for peak power have better spectral as well as power efficiency than those optimized for average power. OOK has the best $\hat{P}_{\text{o, gain}}$ among all studied modulation formats. Further, OOK and $\mathscr{T}_4$ have a better $\eta$ than $\mathscr{C}_4$, $\mathscr{T}_{\hat{P}_{\text{o}},3}$, $\mathscr{T}_{\bar{P}_{\text{o}},3}$, and QPSK. The two-dimensional 8-ary formats have higher $\eta$ than the three-dimensional 16-ary formats, and 4-PAM has the highest $\eta$ and the lowest $\hat{P}_{\text{o, gain}}$ among the studied modulation formats.

*3) $\bar{P}_{\text{o, gain}}$ vs. $\eta$ with $K = 0.99$ (Fig. 5):* As before, modulation formats optimized for average power have a higher $\bar{P}_{\text{o, gain}}$ than those optimized for peak power. $\mathscr{T}_{\bar{P}_{\text{o}},3}$ and $\mathscr{C}_4$ have the highest $\bar{P}_{\text{o, gain}}$ among the studied formats. QPSK and 4-PAM have similar $\eta$ which is the highest among the 2-, 3-, and 4-ary constellations. Unlike the case where $K = 0.9$, the three-dimensional 8-ary constellations are better in spectral and power efficiency in comparison to the two-dimensional 8-ary constellations. In addition, $\mathscr{C}_{\hat{P}_{\text{o}},16}$ has the highest $\eta$ among the studied constellations. The two-dimensional constellations have more power close to DC, whereas the three-dimensional constellations have a wider main lobe. This makes the 99% in-band power for the three-dimensional constellations occur at frequencies lower than those for the two-dimensional ones.

*4) $\hat{P}_{\text{o, gain}}$ vs. $\eta$ with $K = 0.99$ (Fig. 6):* As in the case where $K = 0.9$, OOK has the highest $\hat{P}_{\text{o, gain}}$. $\mathscr{C}_4$ has the same power efficiency as $\mathscr{T}_4$, but has a higher $\eta$. QPSK and 4-PAM, as in the previous case, have similar $\eta$ which is the highest among the 2-, 3-, and 4-ary constellations. The three-dimensional 8- and 16-ary constellations have higher $\eta$ than the two-dimensional formats, and the 16-ary constellation optimized for peak power has the highest $\eta$.

## V. Conclusions

We presented a two-dimensional signal space for IM/DD that provides a good trade-off between implementation complexity and spectral efficiency. This signal space suggests simpler modulator and demodulator structures than for the three-dimensional raised-QAM signal space. For a fractional power bandwidth of $K = 0.9$, the two-dimensional formats have better spectral characteristics than the three-dimensional ones. Therefore, the two-dimensional formats are a good choice for single-wavelength optical systems. However, for a fractional power bandwidth of $K = 0.99$, the three-dimensional formats have better spectral characteristics. Therefore, they are suitable for wavelength-division multiplexing (WDM) systems where crosstalk between adjacent channels is important. For both signal spaces, modulation formats optimized for peak power achieve a higher spectral efficiency than those optimized for average power.

## Appendix A
## Obtained Constellations

Constellations are normalized to unit minimum distance.

$$\mathscr{T}_{\bar{P}_{\text{o}},3} = \{(0,0), (\sqrt{2/3}, \pm 1/\sqrt{3})\}.$$
$$\mathscr{T}_{\hat{P}_{\text{o}},3} = \{(0,0), (\sqrt{3}/2, \pm 1/2)\}.$$
$$\mathscr{T}_4 = \mathscr{T}_{\bar{P}_{\text{o}},3} \cup \{(2\sqrt{2/3}, 0)\}.$$
$$\mathscr{T}_{\bar{P}_{\text{o}},8} = \mathscr{T}_4 \cup \{(2\sqrt{2/3}, \pm 2/\sqrt{3}), (\sqrt{6}, \pm 1/\sqrt{3})\}.$$
$$\mathscr{T}_{\hat{P}_{\text{o}},8} = \mathscr{T}_4 \cup \{(\sqrt{2/3} + \sqrt{3}/2, \pm(1/2 + 1/\sqrt{3})), (2\sqrt{2/3} + \sqrt{3}/2, \pm 1/2)\}.$$

## Acknowledgments

J. Karout and E. Agrell were supported by SSF under grant RE07-0026. G. Kramer was supported by an Alexander von Humboldt Professorship endowed by the German Federal Ministry of Education and Research. F. R. Kschischang was supported by a Hans Fischer Senior Fellowship of the Institute for Advanced Study, Technische Universität München, funded by the German Excellence Initiative. The authors would like to acknowledge R. Krishnan for comments on the paper.

## References

[1] J. R. Barry, *Wireless Infrared Communications*. Norwell, MA, USA: Kluwer Academic Publishers, 1994.

[2] J. M. Kahn and J. R. Barry, "Wireless infrared communications," *Proc. IEEE*, vol. 85, no. 2, pp. 265–298, 1997.

[3] S. Hranilovic, *Wireless Optical Communication Systems*. New York: Springer, 2005.

[4] S. Randel, F. Breyer, and S. C. J. Lee, "High-speed transmission over multimode optical fibers," in *Proc. Opt. Fiber Commun. Conf.*, 2008, p. OWR2.

[5] S. Hranilovic and F. R. Kschischang, "Optical intensity-modulated direct detection channels: Signal space and lattice codes," *IEEE Trans. Inf. Theory*, vol. 49, no. 6, pp. 1385–1399, 2003.

[6] J. Karout, E. Agrell, K. Szczerba, and M. Karlsson, "Designing power-efficient modulation formats for noncoherent optical systems," in *Proc. IEEE Glob. Commun. Conf.*, 2011.

[7] ——, "Optimizing constellations for single-subcarrier intensity-modulated optical systems," *IEEE Trans. Inf. Theory*, 2012, to appear, arXiv:1106.2819.

[8] K.-P. Ho, *Phase-Modulated Optical Communication Systems*. New York: Springer, 2005.

[9] S. Walklin and J. Conradi, "Multilevel signaling for increasing the reach of 10 Gb/s lightwave systems," *J. Lightw. Technol.*, vol. 17, no. 11, pp. 2235–2248, 1999.

[10] M. K. Simon, S. M. Hinedi, and W. C. Lindsey, *Digital Communication Techniques: Signal Design and Detection*. Englewood Cliffs, NJ: Prentice-Hall, 1995.

[11] G. P. Agrawal, *Lightwave Technology: Telecommunication Systems*. New Jersey: John Wiley & Sons, Inc., 2005.

[12] C. Cox and W. S. C. Chang, "Figures of merit and performance analysis of photonic microwave links," in *RF Photonic Technology in Optical Fiber Links*, W. S. C. Chang, Ed. Cambridge University Press, 2002, ch. 1, pp. 1–33.

[13] B. Inan, S. C. J. Lee, S. Randel, I. Neokosmidis, A. M. J. Koonen, and J. W. Walewski, "Impact of LED nonlinearity on discrete multitone modulation," *J. Opt. Commun. Network.*, vol. 1, no. 5, pp. 439–451, Oct. 2009.

[14] T. Aulin and C.-E. W. Sundberg, "Continuous phase modulation—Part I: Full response signaling," *IEEE Trans. Commun.*, vol. COM-29, no. 3, pp. 196–209, Mar. 1981.

[15] S. G. Wilson, *Digital Modulation and Coding*. New Jersey: Prentice-Hall, 1996.